



Herpes Simplex Virus 1 Entry Glycoproteins Form Complexes before and during Membrane Fusion

Zempen Pataki,^{a,b} Andrea Rebolledo Viveros,^{a,b}  Ekaterina E. Heldwein^{a,b}

^aDepartment of Molecular Biology and Microbiology, Tufts University School of Medicine, Boston, Massachusetts, USA

^bGraduate Program in Molecular Microbiology, Graduate School of Biomedical Sciences, Tufts University School of Medicine, Boston, Massachusetts, USA

ABSTRACT Herpesviruses—ubiquitous pathogens that cause persistent infections—have some of the most complex cell entry mechanisms. Entry of the prototypical herpes simplex virus 1 (HSV-1) requires coordinated efforts of 4 glycoproteins, gB, gD, gH, and gL. The current model posits that the glycoproteins do not interact before receptor engagement and that binding of gD to its receptor causes a “cascade” of sequential pairwise interactions, first activating the gH/gL complex and subsequently activating gB, the viral fusogen. But how these glycoproteins interact remains unresolved. Here, using a quantitative split-luciferase approach, we show that pairwise HSV-1 glycoprotein complexes form before fusion, interact at a steady level throughout fusion, and do not depend on the presence of the cellular receptor. Based on our findings, we propose a revised “conformational cascade” model of HSV-1 entry. We hypothesize that all 4 glycoproteins assemble into a complex before fusion, with gH/gL positioned between gD and gB. Once gD binds to a cognate receptor, the proximity of the glycoproteins within this complex allows for efficient transmission of the activating signal from the receptor-activated gD to gH/gL to gB through sequential conformational changes, ultimately triggering the fusogenic refolding of gB. Our results also highlight previously unappreciated contributions of the transmembrane and cytoplasmic domains to glycoprotein interactions and fusion. Similar principles could be at play in other multicomponent viral entry systems, and the split-luciferase approach used here is a powerful tool for investigating protein-protein interactions in these and a variety of other systems.

IMPORTANCE Herpes simplex virus 1 (HSV-1) infects the majority of humans for life and can cause diseases ranging from painful sores to deadly brain inflammation. No vaccines or curative treatments currently exist. HSV-1 infection of target cells requires coordinated efforts of four viral glycoproteins. But how these glycoproteins interact remains unclear. Using a quantitative protein interaction assay, we found that HSV-1 glycoproteins form receptor-independent complexes and interact at a steady level. We propose that the 4 proteins form a complex, which could facilitate transmission of the entry-triggering signal from the receptor-binding component to the membrane fusogen component through sequential conformational changes. Similar principles could be applicable across other multicomponent protein systems. A revised model of HSV-1 entry could facilitate the development of therapeutics targeting this process.

KEYWORDS herpesvirus, HSV-1, interaction, domain, membrane fusion, glycoprotein, chimeric protein, NanoBiT protein interaction assay, split-luciferase cell-cell fusion assay

Enveloped viruses enter cells by fusing their membrane envelope with a cellular membrane, and most use a single viral protein, termed a fusogen, to perform this function. Fusogens bridge apposing membranes and merge them by refolding from the high-energy prefusion conformation into a lower-energy postfusion conformation. The energy released during these favorable conformational rearrangements is thought to overcome the activation energy of the membrane fusion process (reviewed in reference 1). Fusogens

Editor Blossom Damania, University of North Carolina, Chapel Hill

Copyright © 2022 Pataki et al. This is an open-access article distributed under the terms of the [Creative Commons Attribution 4.0 International license](https://creativecommons.org/licenses/by/4.0/).

Address correspondence to Ekaterina E. Heldwein, katya.heldwein@tufts.edu.

The authors declare no conflict of interest.

This article is a direct contribution from Ekaterina E. Heldwein, a Fellow of the American Academy of Microbiology, who arranged for and secured reviews by Richard Longnecker, Northwestern University Feinberg School of Medicine, and Sarah Connolly, DePaul University.

Received 18 July 2022

Accepted 25 July 2022

Published 16 August 2022

are commonly activated, or triggered, by either exposure to low pH or by binding to a receptor on the target cell (reviewed in reference 1). In herpesviruses, the fusion mechanism is more complex, however, and requires three or more viral proteins that join forces to bring about fusion (reviewed in reference 2). These double-stranded DNA viruses are significant pathogens that establish lifelong infections (reviewed in reference 3). Herpes simplex virus 1 (HSV-1), the focus of this study, is a prototypical herpesvirus (reviewed in reference 4) that infects ~67% of people under the age of 50 worldwide (5) and causes ailments ranging from oral sores (reviewed in reference 6) to encephalitis (reviewed in reference 7–9). As there is no curative treatment (reviewed in references 10) or vaccines for HSV-1 (11), a better understanding of HSV-1 biology is essential for combating the global burden of HSV-1 disease.

Glycoprotein B (gB) is the conserved fusogen in herpesviruses. By analogy with other fusogens, this homotrimeric protein is thought to merge membranes by refolding from the prefusion (12, 13) to the postfusion conformation (14–18). However, gB is not a stand-alone fusogen and must be activated by a complex of two conserved viral glycoproteins, gH and gL (although some mutant gB forms can mediate fusion independently, albeit at a reduced level [19, 20]). In some cases, such as in Kaposi Sarcoma-associated herpesvirus (KSHV) (21, 22) or varicella zoster virus (VZV) (23) or during Epstein-Barr virus (EBV) infection of epithelial cells (24), gH/gL activates gB upon binding to a cognate host cell receptor directly (reviewed in references 2 and 25). In other cases, such as HSV or human cytomegalovirus (HCMV) or during EBV infection of B cells, gH/gL instead detects the host cell receptor indirectly by binding to an accessory viral protein (reviewed in references 2 and 25), e.g., gD in HSV-1 and 2 (26, 27; reviewed in reference 28), UL128/UL130/UL131A or gO in HCMV (29–31), and gp42 in EBV (32). How these multiple glycoproteins interact to bring about fusion is a key question that has not yet been fully answered. While structures of gH/gL bound to accessory viral proteins have been determined for EBV (33) and HCMV (34, 35), and the gH/gL-gB complex in HCMV has been captured by coimmunoprecipitation (36) and visualized at low resolution (37), very little is known about how HSV-1 gD, gH/gL, and gB interact.

HSV-1 gD, gH, and gB are transmembrane proteins that consist of extracellular domains, or ectodomains, single-spanning transmembrane domains (TMD), and cytoplasmic domains (CTD or CT), whereas gL is a soluble protein that binds the gH ectodomain. Any of these domains could, in principle, mediate mutual interactions. Indeed, purified recombinant HSV-1 gD and gH/gL ectodomains have been reported to bind *in vitro* in a surface plasmon experiment (38, 39). Pairwise gD-gH/gL, gD-gB, and gH/gL-gB interactions have also been detected in live cells, by C-terminally tagging each interacting partner with a split-fluorescent protein (40, 41). However, the split-fluorescent protein approach was not used quantitatively in these studies and has yielded some contradictory results, with some reports suggesting that gH/gL-gB interaction requires the presence of gD and receptor (40, 41) and others maintaining that it does not (42). Moreover, another study using the split-fluorescent protein approach detected interactions of the HSV glycoproteins gD, gH/gL, and gB with glycoproteins from an unrelated paramyxovirus (43). This suggested that the high-affinity, irreversible interactions of the split-fluorescent protein fragments can drive nonspecific interactions between tagged proteins (43 and reviewed in reference 44). Therefore, the extent and timing of interactions between HSV-1 gD, gH/gL, and gB in live cells remains unclear.

Based on these prior studies, two models have emerged to explain how the glycoproteins activate one another for membrane fusion. One model is that the viral glycoproteins do not interact until gD binds to a receptor, and then gD binds to gH/gL followed by gH/gL binding to gB for sequential activation (Fig. 1) (40, 45, 46). Alternatively, gD, gH/gL, and gB are already bound to one another, and when a receptor binds to gD, activating signals are transmitted from gD to gH/gL to gB (42). In both models, the sequential activation of gD, gH/gL, and gB likely involves conformational changes of the glycoproteins (12, 15, 38, 47 and reviewed in reference 48).

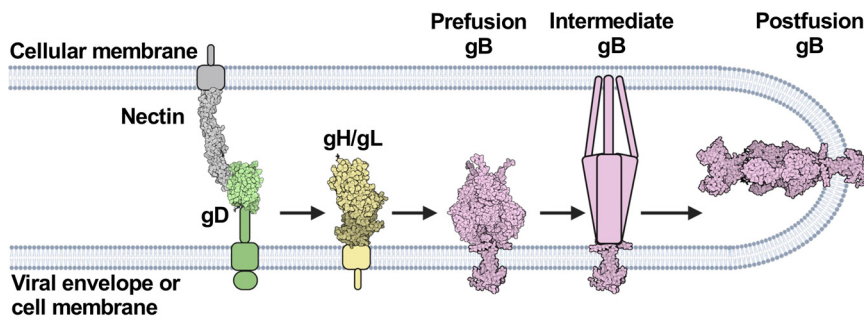


FIG 1 HSV-1 fusion pathway model. gD (PDB 2C36) (72) binds a receptor (PDB 3U83) (77) on the target cell. gD then activates gH/gL; gH/gL (PDB 3M1C) (78) activates gB (PDB 6Z9M and 5V2S) (12, 15) to refold and cause membrane fusion. gD is thought to be a dimer (72) but is shown here as a monomer for clarity. Figure created with [BioRender.com](https://www.biorender.com).

Here, to clarify the timing, dynamics, and sites of interactions between gD, gH/gL, and gB, we turned to a quantitative protein-protein interaction technique called NanoBiT that uses split-luciferase fragments fused to putative interaction partners in live cells (49). Unlike split-fluorescent protein fragments, the split-luciferase fragments interact in a low-affinity, reversible manner, which reduces the likelihood of false positives and allows the detection of not only complex association but also dissociation over time.

We found that gD-gH/gL, gH/gL-gB, and gD-gB interactions were independent of the presence of the receptor nectin-1 and were steady, which suggested that these glycoprotein complexes formed before fusion and were maintained throughout fusion. By replacing the HSV-1 gH/gL domains with those of EBV gH or a scrambled sequence, we found that gD-gH/gL and gH/gL-gB interactions involved all three major domains of gH (ectodomain, TMD, and CT). However, while the HSV-1 gH TMD or CT each mediated efficient formation of the gD-gH/gL and gH/gL-gB complexes, the HSV-1 gH ectodomain did not. Therefore, the HSV-1 gH TMD and CT are more important for interactions with gD and gB than the ectodomain. In contrast, all HSV-1 gH/gL domains were essential for fusion, suggesting that glycoprotein complex formation is not sufficient for fusion. Finally, our data indicate that whereas gH and gB interact in the endoplasmic reticulum (ER), gH and gD do not.

Putting these findings together, we propose a revised model of HSV-1-mediated fusion whereby a proportion of gH/gL and gB associate in the ER and are transported to the plasma membrane together, whereas gD traffics there independently. Once at the plasma membrane, gD, gH/gL, and gB form a complex. When gD binds to a cognate receptor, the proximity of the glycoproteins within this complex allows for efficient transmission of the activating signal from gD to gH/gL and from gH/gL to gB through conformational changes, in a “conformational cascade.” Our findings increase our understanding of the HSV-1 fusion pathway and may pinpoint new targets for inhibition of HSV-1 infection.

RESULTS

Tagging HSV-1 gH/gL and gB with split luciferases to probe their interaction.

To examine the timing and duration of glycoprotein interactions in HSV-1, we turned to a split-luciferase (NanoBiT) interaction assay in live cells (49). In this assay, two proteins of interest are tagged with complementary parts of a split luciferase, Lg-BiT and Sm-BiT, and if they interact, the active luciferase is formed, and the resulting luminescence reports on the interaction (Fig. 2a). To begin with, gH and gB were C-terminally tagged with Lg-BiT or Sm-BiT (gH-Lg and gB-Sm or gH-Sm and gB-Lg). In initial studies, the gH-Lg/gB-Sm combination resulted in a higher signal-to-noise ratio in the NanoBiT assay than the gH-Sm/gB-Lg combination, so the former combination was chosen for our experiments, as recommended in the NanoBiT technical manual (50). We also used the gB-Sm/gB-Lg combination in our experiments as a positive control because gB forms trimers. gH-Lg/gL, gB-Sm, and gB-Lg

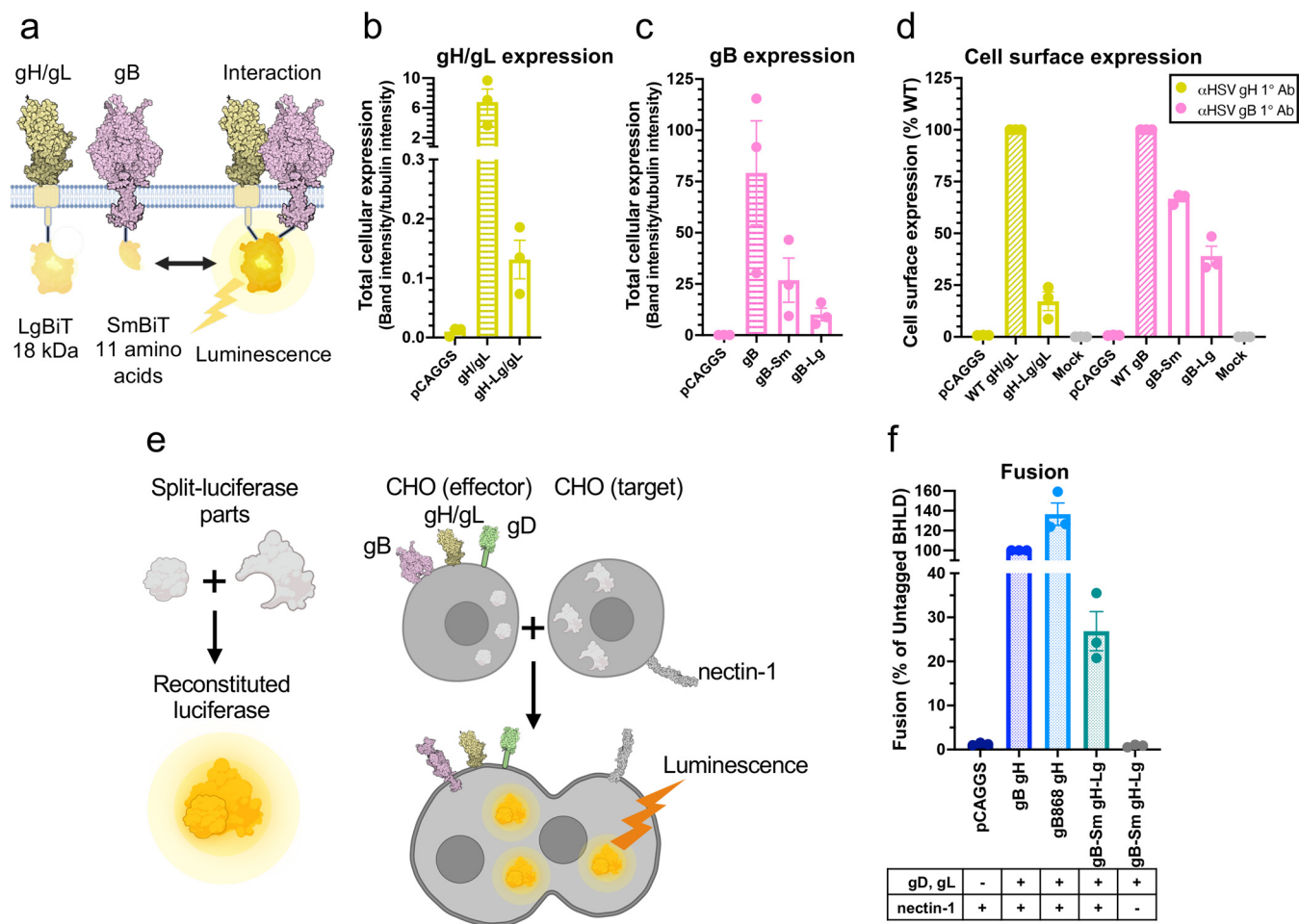


FIG 2 Tagging HSV-1 gH/gL and gB with split luciferases to probe their interaction. (a) NanoBIT protein-protein interaction assay approach (49). The interaction between gH/gL and gB was tested by tagging gH and gB with complementary parts of a split luciferase and transfecting into cells. Reconstitution of luciferase reports on fusion. (b to d) Total cellular expression and cell-surface expression of Lg- and Sm- tagged gH and gB by Western blotting and flow cytometry, respectively. R137 and R68 antibodies for gH/gL and gB for Western blotting, respectively. LP11 and R68 antibodies for gH/gL and gB for flow cytometry, respectively. pCAGGS was an empty vector negative control. The mock control was an untransfected negative control, incubated with a nontargeting primary antibody. Columns show the mean. Error bars are the standard error of the mean (SEM). (e) Split-luciferase cell-cell fusion assay (51) experimental setup to test whether tagged proteins retain their function. Cells transfected with viral proteins fuse to cells transfected with nectin-1 receptor. Reconstitution of RLuc8 luciferase reports on fusion. (b) Total fusion of gB-Sm and gH-Lg/Lg, 8 h after mixing effector and target cells. gB868 was a hyperfusogenic positive-control gB construct. pCAGGS and the condition without nectin-1 receptor are negative controls. Columns show the mean. Error bars are the SEM. Data are three biological replicates from independent experiments. Diagrams and cartoons were created using [BioRender.com](https://www.biorender.com).

had a significantly lower total cellular expression than untagged gH/gL and gB (Fig. 2b and c), with the Lg tag reducing expression more than the Sm tag. gH-Lg/gL, gB-Sm, and gB-Lg were expressed on the cell surface, however, indicating that they were properly folded and transported to the cell surface (Fig. 2d). The difference in total cellular expression between wild-type (WT) and BiT-tagged constructs was much greater than the difference in their cell surface expression. In other words, the BiT-tagged constructs had relatively high cell surface expression compared to their total cellular expression (Fig. 2b to d). In contrast, the WT gH/gL and gB constructs have a relatively low cell surface expression compared to their total cellular expression, which we attribute to protein overexpression. We note that low overall expression levels of gH-Lg/gL and gB-Sm are advantageous because they reduce the potential for nonspecific association between interaction partners (50).

To evaluate the gH/gL-gB interaction not only before but also during fusion, we tested whether gH-Lg/gL and gB-Sm could mediate membrane fusion under conditions that closely mimic the NanoBIT interaction assay conditions. We measured cell-cell fusion using a split Renilla luciferase (RLuc8) cell-cell fusion assay (51). In this assay, “effector” cells are transfected with gD, gH, gL, gB, and one part of a split luciferase,

whereas “target” cells are transfected with the nectin-1 receptor and the complementary part of the split luciferase. Effector and target cells are then mixed, and cell-cell fusion is measured by the luminescence produced upon reconstitution of the luciferase (Fig. 2e). The RLuc8 luciferase used for the cell-cell fusion assay is different from the NanoBiT luciferase and uses EnduRen as a substrate instead of Endurazine. Fusion of HSV-1 gH-Lg and gB-Sm (in the presence of HSV-1 gD, gL, and nectin-1) was 27% of that of untagged HSV-1 proteins, indicating that the NanoBiT tags do not abrogate the fusion function of gH and gB (Fig. 2f). Decreased fusion extent was likely due to the lower cell surface expression of HSV-1 gH-Lg/gL (17% of the untagged HSV-1 gH/gL) and gB-Sm (67% of the untagged HSV-1 gB) (Fig. 2d). Fusion levels were similar to those of the negative control in the presence of receptor-negative target cells, which confirmed that the NanoBiT luciferase activity was not responsible for the luminescence signal measured during the cell-cell fusion assay (Fig. 2e).

HSV-1 gH/gL and gB interact at a steady level and independently of nectin-1.

Interaction between gH/gL and gB was measured before and during fusion that was initiated by the addition of target cells expressing the HSV-1 receptor nectin-1 (Fig. 3a). The assay conditions were the same as for the cell-cell fusion assay except that the split RLuc8 luciferase fragments were not transfected and the NanoBiT luciferase substrate was used. Sm-BiT fused to HaloTag (Halo-Sm), which is unlikely to interact with gH, was used as a negative control in the interaction assay. HaloTag is a cytoplasmic protein derived from a bacterial haloalkane dehalogenase enzyme unrelated to viral glycoproteins (reviewed in reference 52). gH/gL from Epstein-Barr virus (EBV) was tagged with Lg-BiT as another negative control. EBV is a gammaherpesvirus that is distantly related to HSV-1, an alphaherpesvirus, so EBV gH/gL was not expected to interact with HSV-1 gB. Indeed, HSV-1 gB does not mediate cell-cell fusion when paired with EBV gH/gL and vice versa (53). HSV gB-Sm and gB-Lg were used as positive controls. NanoBiT-tagged protein kinase A catalytic (PRKACA) and type 2A regulatory (PRKAR2A) subunits, known to interact, served as other positive controls (49). Luciferase substrate was added directly before the luminescence measurements were begun. It takes a few hours after substrate addition to reach maximum luminescence signal, after which there is slight signal decay from substrate turnover (54). We found that HSV-1 gH-Lg/gL and gB-Sm interact at a steady level before and during fusion (Fig. 3b and c). gH/gL-gB interaction was detected in the absence of the target cells, and no noticeable change in gH/gL-gB interaction was seen upon addition of nectin-1-expressing target cells (Fig. 3b). Further, the extent of interaction was similar regardless of the presence of nectin-1 in target cells (Fig. 3c). We conclude that under these experimental conditions, HSV-1 gH/gL and gB form a complex that exists at a steady level and does not require gD-nectin-1 interaction. EBV gH-Lg/gL did not interact with HSV gB-Sm, whereas HSV gB-Sm interacted with gB-Lg, as expected (Fig. 3b and c).

HSV-1 gH/gL interacts with both prefusion and postfusion forms of HSV-1 gB.

Our results suggested that gH/gL and gB interact but left unclear whether gH/gL interacted with the prefusion, postfusion, or both conformations of gB because gB exists as a mixture of these two conformations on the cell surface (55–57) and on virions (58). Therefore, we introduced the H516P mutation into gB-Sm, which has been reported to stabilize gB in its prefusion conformation (12). The gB-Sm H516P mutant had similar total cellular expression as the WT gB-Sm (Fig. 3d) and was expressed on the cell surface (Fig. 3e). The gB-Sm H516P mutant interacted with gH/gL to a similar extent as the WT gB-Sm (Fig. 3f), indicating that gH/gL can interact with prefusion gB, and therefore, that the gH/gL-gB interaction occurs before fusion. Although there is no known gB mutation that stabilizes its postfusion conformation, we hypothesize that gH/gL likely also interacts with postfusion gB because the gH/gL-gB interaction remains at a steady level as fusion progresses, even as the prefusion form converts into the postfusion form.

All HSV-1 gH domains are involved in interactions with HSV-1 gB, but the TMD and the CT are more important than the ectodomain. Having observed a steady gH/gL-gB interaction, we sought to identify the gH domains that were involved in it. Toward this goal, we created gH-Lg variants to disrupt interactions between domains.

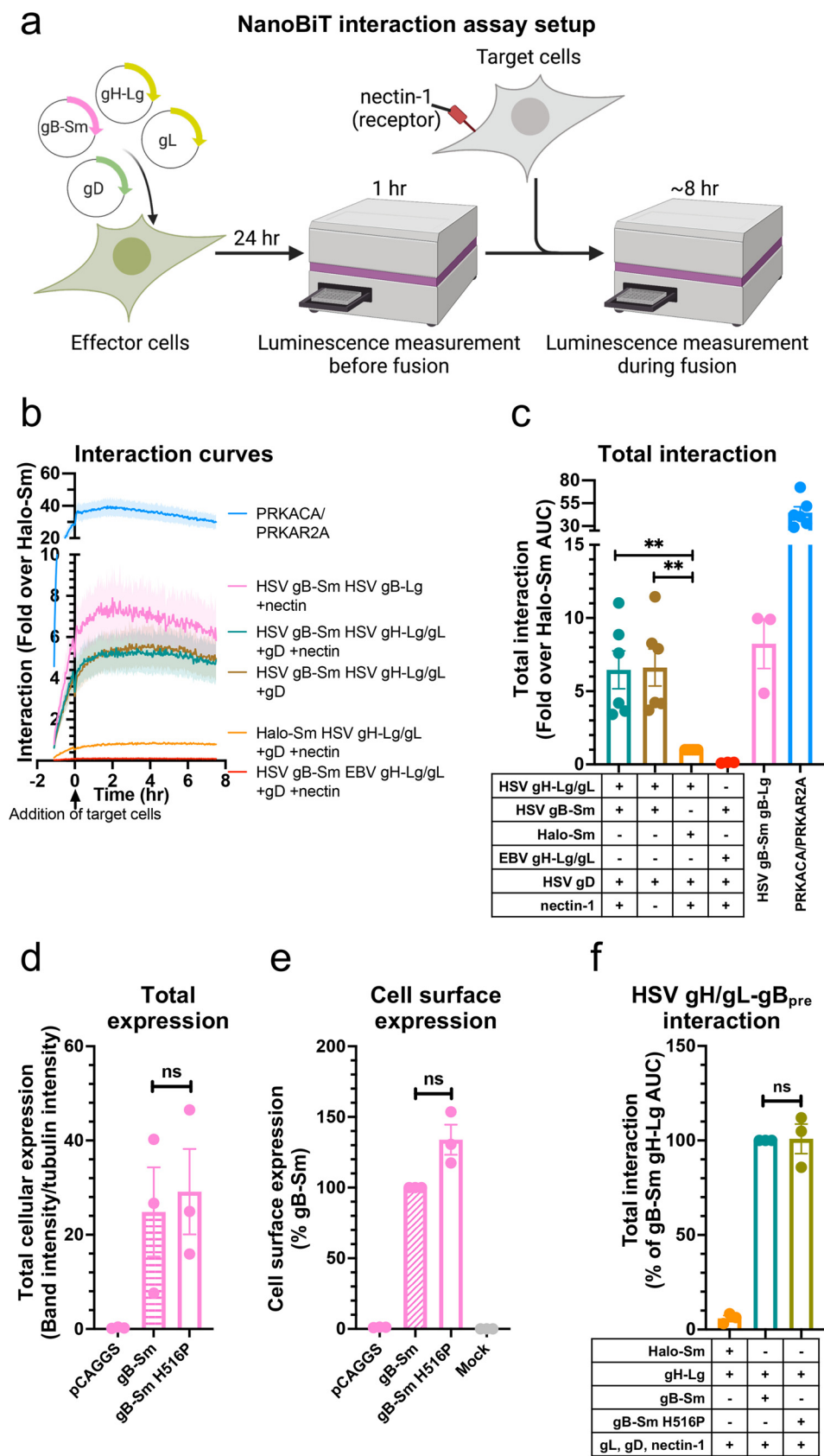


FIG 3 HSV-1 gH/gL and gB interact at a steady level and independently of nectin-1. (a) Interaction assay experimental setup. Cells are transfected with viral proteins required for fusion, including split-luciferase-tagged (Continued on next page)

To disrupt interactions between the ectodomains or TMDs, we replaced the ectodomain or TMD of HSV-1 gH with those of gH from EBV (Fig. 4a, constructs 6 and 3, respectively). EBV is a gammaherpesvirus that is distantly related to HSV-1, an alpha-herpesvirus, so EBV gH/gL is not expected to interact with HSV-1 gB. To enable proper folding, gH chimeras containing HSV-1 gH ectodomain were coexpressed with HSV-1 gL, whereas those containing EBV gH ectodomain were coexpressed with EBV gL. To disrupt interactions between the gB CTD and gH CT, the HSV-1 gH CT was scrambled by arranging its amino acids in a random order (Fig. 4a, construct 4). This method was chosen instead of replacing the HSV-1 gH CT with that of EBV gH because we reasoned that the scrambled HSV-1 gH CT was less likely to interact with the HSV-1 gB CTD than the EBV gH CT, which shares sequence similarity with the HSV-1 gH CT (Fig. 4b). For example, the EBV gH CT has two hydrophobic amino acid clusters, KIV and FFL, which are similar to the KVL and FFW clusters in the HSV-1 gH CT (Fig. 4b). Additional constructs were also generated to disrupt interactions in two domains simultaneously (Fig. 4a, constructs 5, 7, and 8). Finally, the full-length EBV gH-Lg/gL construct was again used as a negative control (Fig. 4a, construct 1).

To rule out the possibility that differences in the expression levels of the gH-Lg/gL constructs could account for differences in their interactions with HSV-1 gB, we measured their total cellular expression. Total cellular expression was measured because gH/gL and gB may interact not only on the cell surface but also at intracellular locations, e.g., in the ER and Golgi. Indeed, it has been shown that gB and gH/gL from HCMV, a betaherpesvirus, can interact in the ER (36). The total cellular expression of the gH-Lg/gL constructs was not statistically significantly different from HSV-1 gH-Lg/gL and EBV gH-Lg/gL (Fig. 4c and d), so differences in protein expression are not expected to account for any differences in interaction with HSV-1 gB among the constructs. All constructs were expressed on the cell surface (Fig. 4e), suggesting that they were properly folded.

When single HSV-1 gH domains were replaced, interactions either remained at a WT HSV-1 gH-Lg/gL level (ECTO_{EBV}; Fig. 4f, construct 6) or were reduced to ~60%, albeit not to a statistically significant extent (TMD_{EBV} and CT_{SCR} constructs; Fig. 4f, constructs 3 and 4). We then tested gH constructs in which two domains were replaced simultaneously. When both the gH TMD and CT were replaced (TMD_{EBV}-CT_{SCR}; Fig. 4f, construct 5), interaction decreased to 54%, indicating that when only the gH ectodomain is from HSV-1, gH/gL-gB interaction cannot be maintained at the WT level. Surprisingly, when both the gH ectodomain and TMD, or both the gH ectodomain and CT, were replaced simultaneously, interactions increased ~2-fold (ECTO_{EBV}-TMD_{EBV} and ECTO_{EBV}-CT_{SCR}; Fig. 4f, constructs 7 and 8). We conclude that although all gH domains appear to be involved in interactions with gB, when only the TMD or the CT is from HSV-1, they are sufficient to maintain WT-level interactions, whereas the ectodomain is not.

All three gH domains are required for fusion. While the TMD or the CT of HSV-1 gH appears sufficient for maintaining WT-level interactions with gB when the rest of the domains are replaced with their EBV gH counterparts or scrambled, it is unlikely that these HSV-1 domains would be sufficient for fusion. To examine this, we tested some of the gH-Lg constructs described above for their ability to support fusion using the cell-cell fusion assay (51). Unlike the WT HSV-1 gH-Lg/gL (Fig. 4g, construct 2), none of the gH-Lg/gL mutant constructs (Fig. 4g, constructs 3, 4, and 6) were able to

FIG 3 Legend (Continued)

proteins of interest. Interaction is measured by luminescence before and during fusion. Fusion is induced by the addition of target cells expressing the viral receptor nectin-1. (b) gH/gL and gB interaction over time, with target cells expressing or lacking nectin-1. The Halo-Sm and EBV gH-Lg conditions were negative controls. gB-Sm/gB-Lg and PRKACA/PRKAR2A were positive controls. The shaded regions are the SEM. (c) The interactions are quantified by calculating the area under the curve (AUC). (d and e) Total cellular expression and cell-surface expression of Sm-tagged gB H516P—which locks gB in its prefusion conformation—by Western blotting and flow cytometry, respectively. (f) The interaction between gH/gL and gB H516P. Columns show the mean. Error bars are the SEM. ns, not statistically significant; **, $P < 0.01$. Data in all panels are three biological replicates from independent experiments. Diagrams were created with [BioRender.com](https://www.biorender.com).

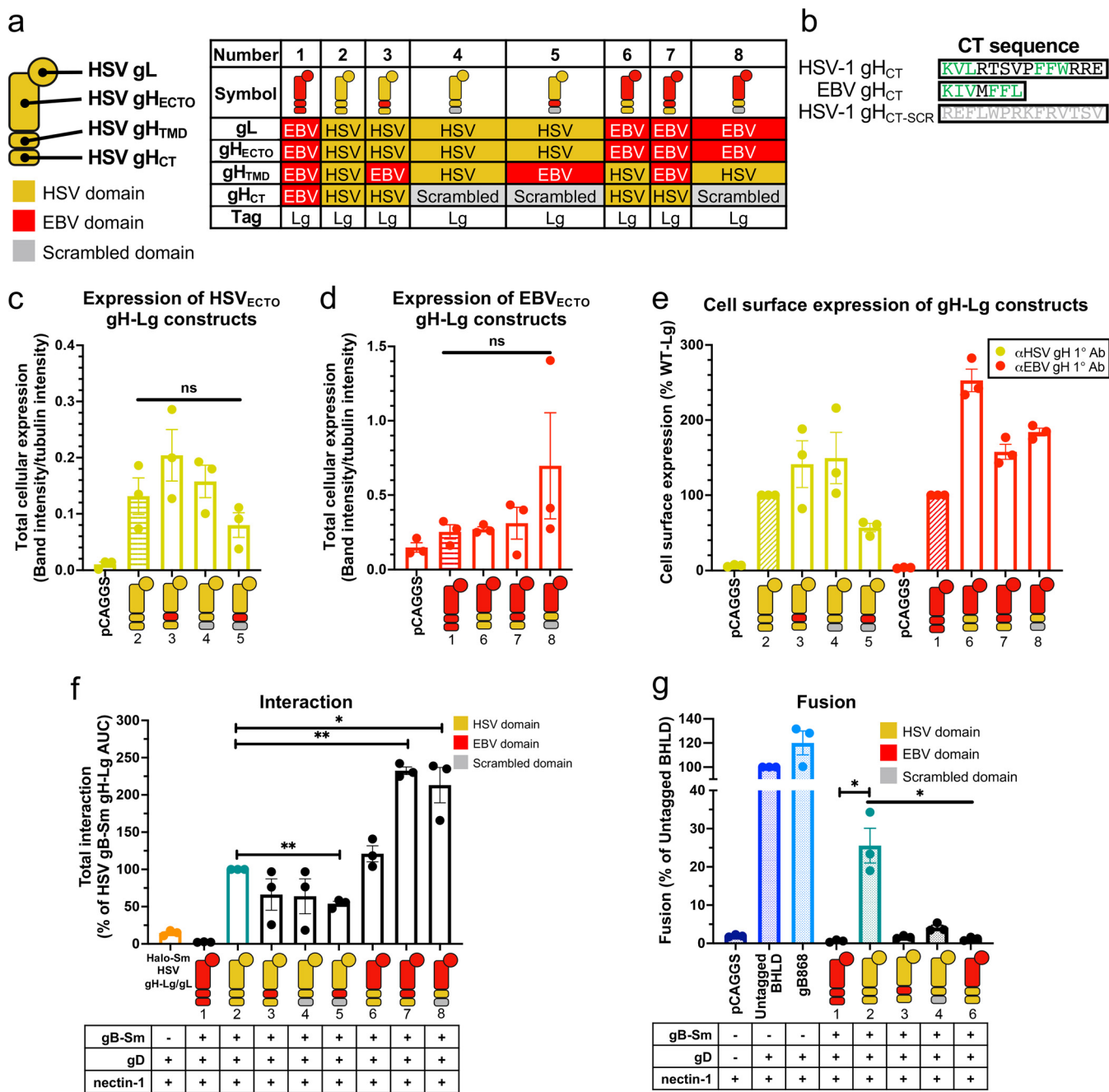


FIG 4 All HSV-1 gH domains are involved in interactions with HSV-1 gB. (a) Summary of the composition of gH-Lg/gL constructs designed to disrupt domain interactions. (b) Sequence comparison of HSV-1, EBV, and scrambled HSV-1 gH cytotails. Green indicates similar clusters of residues in HSV-1 and EBV. (c and d) Total cellular expression of gH-Lg/gL constructs with disrupted domain interactions compared to HSV gH-Lg/gL (2) or EBV gH-Lg/gL (1). Cartoons represent gH-Lg/gL constructs, indicating which domains are HSV-1 (yellow), EBV (red), or scrambled (grey). R137 and R2267 antibodies were used against constructs with HSV and EBV ectodomains, respectively. (e) Cell surface expression of gH-Lg/gL constructs with disrupted domain interactions. LP11 and AMMO1 antibodies were used against constructs with HSV and EBV ectodomains, respectively. (f) Interaction between gB and gH/gL constructs with disrupted ectodomain, TMD, or CTD interactions. (g) Total fusion of gB-Sm and gH-Lg/gL constructs with disrupted domain interactions 8 h after mixing effector and target cells. Columns show the mean. Error bars are the SEM. *, $P < 0.05$; **, $P < 0.01$. Data in all panels are three biological replicates from independent experiments. Cartoons were created using [BioRender.com](https://www.biorender.com).

support fusion. Thus, interaction between gH/gL and gB is not sufficient for fusion, and all three HSV-1 gH domains are required for fusion.

HSV-1 gH/gL and gD interact at a steady level and independently of nectin-1.

The regulatory cascade model of HSV-1-mediated membrane fusion (Fig. 1) is

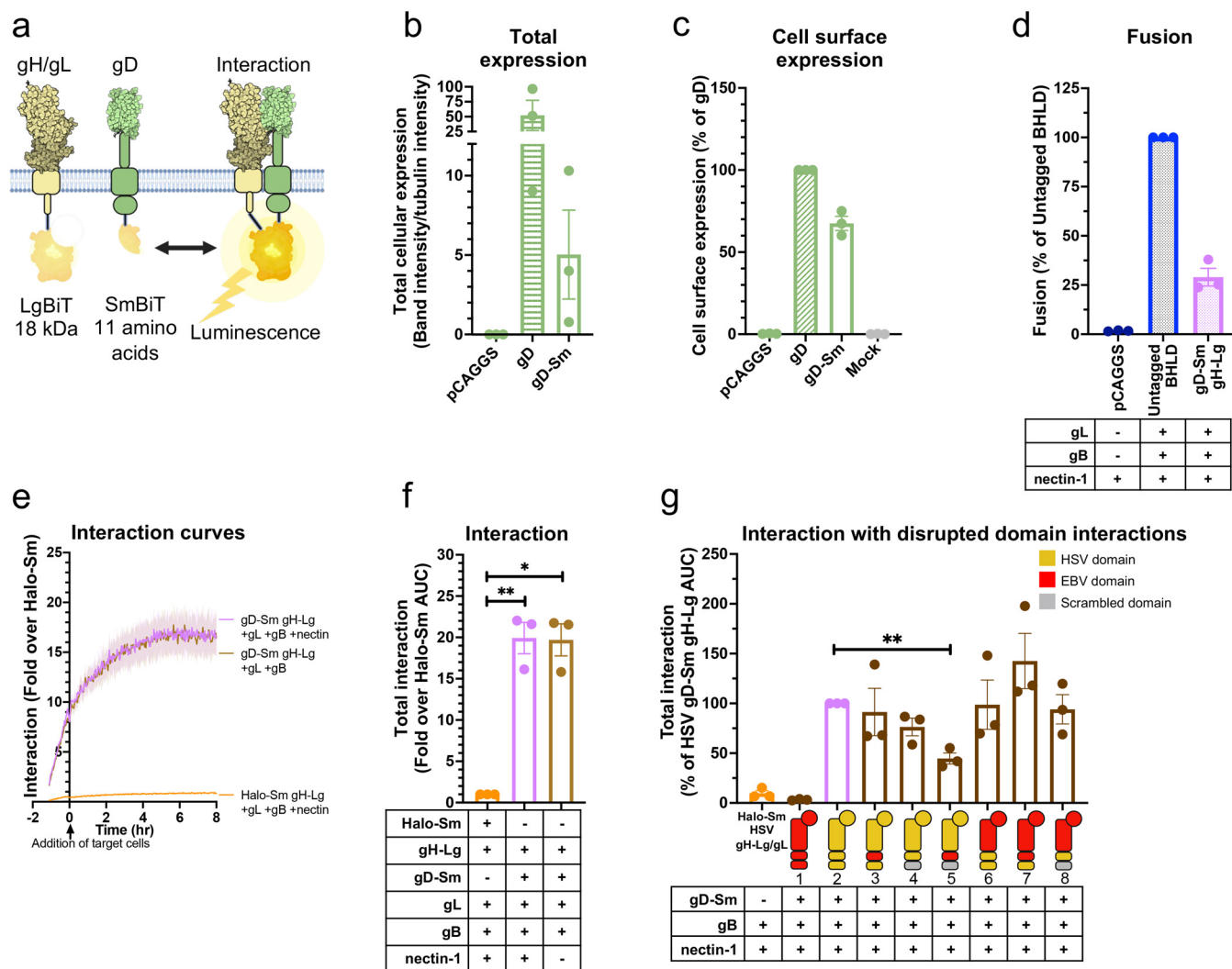


FIG 5 HSV-1 gH/gL and gD interact at a steady level and independently of nectin-1, through all domains. (a) NanoBiT interaction assay setup to test gD-gH/gL interactions. (b and c) Total cellular expression and cell surface expression of gD-Sm by Western blotting and flow cytometry, respectively. R7 and DL6 antibodies were used, respectively. (d) Total fusion of gD-Sm and gH-Lg/gL. (e and f) Interaction of gD and gH/gL. Curves or bars represent the mean, and the shaded area or error bars are the SEM. (g) Interaction of gD with gH/gL with disrupted domain interactions. Columns are the mean, and error bars are the SEM. *, $P < 0.05$; **, $P < 0.01$. Data in all panels are three biological replicates from independent experiments. Illustrations were created with BioRender.com.

predicated upon both gH/gL-gB and gD-gH/gL interactions. To probe the gD-gH/gL interaction and the role of the receptor in it, we generated the gD-Sm construct to test its interaction with gH-Lg/gL (Fig. 5a). gD-Sm had reduced total cellular expression relative to the untagged gD (Fig. 5b). This is consistent with the expression levels of other NanoBiT-tagged constructs and is advantageous because low expression reduces the likelihood of nonspecific interactions. gD-Sm was expressed on the cell surface at 68% of the untagged HSV-1 gD (Fig. 5c) and supported fusion in combination with gH-Lg at 29% of that of untagged HSV-1 proteins (Fig. 5d), indicating that the NanoBiT tag does not abrogate the fusion function of gD. We found that gD-Sm interacted with gH-Lg/gL at a steady level before and during fusion and that the presence of nectin-1 had no apparent effect on the interaction (Fig. 5e and f). We conclude that under these experimental conditions, HSV-1 gD and gH/gL form a complex that exists at a steady level and does not require gD-nectin-1 interaction.

All HSV-1 gH domains are involved in interactions with HSV-1 gD, but the TMD and the CT are more important than the ectodomain. To identify gH domains important for the gD-gH/gL interaction, we tested the interaction of gD-Sm with the same

series of gH-Lg/gL constructs that were used to probe the gH/gL-gB interaction. As expected, EBV gH-Lg/gL did not interact with HSV-1 gD-Sm (Fig. 5g). All but one gH-Lg construct interacted with HSV-1 gD-Sm at a WT HSV-1 gH-Lg level, with no statistically significant differences. Only the construct in which both the gH TMD and CT were replaced (TMD_{EBV}-CT_{SCR1}; Fig. 5g, construct 5) had a significantly decreased interaction, to 45% of that of WT HSV-1 gH-Lg. Thus, we conclude that although all gH domains are involved in interactions with gD, the TMD or the CT from HSV-1 are sufficient to maintain WT-level interactions, whereas the ectodomain is not.

HSV-1 gD and gB interact at a steady level and independently of nectin-1. Since HSV-1 gH/gL interacted at a steady level with both HSV-1 gB and gD, we asked whether gD and gB could also interact. Thus, we generated HSV-1 gD-Lg to test its interaction with gB-Sm (Fig. 6a). Similarly to the tagged gH and gB constructs, gD-Lg had low total cellular expression (Fig. 6b), was expressed on the cell surface at 12% of the untagged HSV-1 gD (Fig. 6c), and supported cell-cell fusion in combination with gB-Sm at 22% of that of untagged HSV-1 proteins (Fig. 6d). We found that gD-Lg interacted with gB-Sm at a steady level before and during fusion and that the presence of nectin-1 had no apparent effect on the interaction (Fig. 6e and f). We conclude that under these experimental conditions, HSV-1 gD and gB form a complex that exists at a steady level and does not require gD-nectin-1 interaction.

HSV-1 gD, gH/gL, and gB compete with one another for binding. So far, we have shown that HSV-1 gD, gH/gL, and gB interact with one another in a pairwise manner. However, in all these experiments, all four HSV-1 glycoproteins were present, leaving unclear whether these pairwise interactions required the presence of the third partner. For example, the gD-gB interaction could require the presence of gH/gL. Alternatively, gD, gH/gL, and gB could compete with one another for binding. To differentiate these possibilities, we tested all pairwise interactions in the absence of the third interacting partner. We detected all three complexes, gD-gH/gL, gH/gL-gB, and gD-gB, even in the absence of the third interacting partner (Fig. 7a to c). Moreover, we found that all three interactions were reduced in the presence of the third partner, but to a different extent. Whereas gD-gH/gL and gH/gL-gB interactions were minimally reduced in the presence of gB or gD, respectively (Fig. 7a and b), the gD-gB interaction was reduced ~3-fold in the presence of gH/gL (Fig. 7c). The observed inhibitory effects are likely due to competition for binding (Fig. 7d). Nonetheless, we cannot exclude the possibility that changes in interaction were due to changes in total cellular expression of the glycoproteins in the presence versus the absence of the third interacting partner.

HSV-1 gL is important for gH-gB and gD-gH interactions and for cell surface expression of gH and gB. gL is thought to be required for transport of gH to the cell surface (59). We confirmed that the total cellular expression levels of gH-Lg were similar in the presence or absence of gL (Fig. 8a) and that gH was not expressed on the cell surface without gL (Fig. 8b). Next, we examined the location of gD-gH and gH-gB interactions. In the absence of gL, gH localizes to the ER (60). Therefore, if gD-gH and gH-gB interactions occurred only on the cell surface, they would no longer be detectable in the absence of gL. Conversely, if interactions occurred in the ER, they could be maintained in the absence of gL. We found that, in the absence of HSV-1 gL, the gD-gH interaction reduced nearly to background levels, ~6-fold (Fig. 8c), which suggested that gD and gH/gL interact mainly on the cell surface. In contrast, in the absence of gL, the gH-gB interaction decreased ~2-fold (Fig. 8d), suggesting that gH and gB can interact in the ER at ~50% of the level of gH/gL-gB interactions under our experimental conditions.

Since in the absence of gL, gH is unable to leave the ER yet can still interact with gB, we next tested whether the gH-gB interaction can also prevent gB from leaving the ER to traffic to the cell surface. Indeed, the gB cell surface expression decreased to 68% in the presence of gH alone relative to when both gH and gL were present (Fig. 8e). In contrast, the gD cell surface expression was not noticeably affected by the absence of gL (Fig. 8f). We conclude that gH and gB can interact in the ER and that gH/gL and gB may traffic together to the cell surface, whereas gH and gD do not interact in the ER to

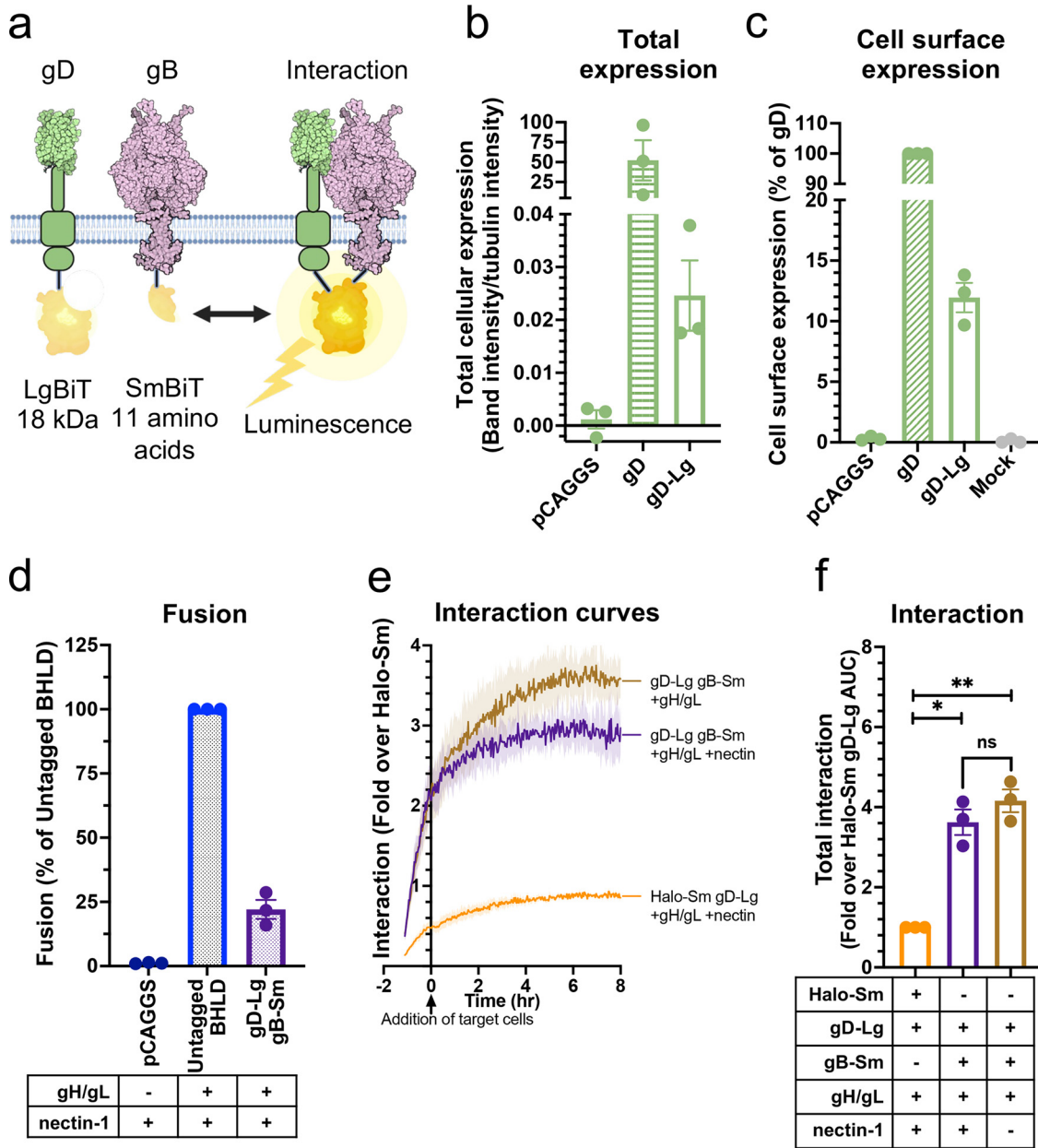


FIG 6 gD and gB interact at a steady level and independently of nectin-1. (a) NanoBiT interaction assay setup to test gD-gB interactions. Created with BioRender.com. (b and c) Total cellular expression and cell surface expression of gD-Lg by Western blotting and flow cytometry, respectively. (d) Total fusion of gD-Lg and gB-Sm. (e and f) Interaction of gD and gB. Curves indicate the mean and the shaded area is the SEM. Columns are the mean and error bars are the SEM. *, $P < 0.05$; **, $P < 0.01$. Data in all panels are three biological replicates from independent experiments.

any significant extent and traffic to the surface independently from one another (Fig. 9a).

DISCUSSION

Interactions between gD, gH/gL, and gB occur before and during fusion. Using the NanoBiT interaction assay, which uses split luciferase (49), we established the timing, duration, and dynamics of the interactions between HSV-1 gD, gH/gL, and gB. The advantage of the NanoBiT interaction assay over the commonly used split-fluorescent proteins is that the split luciferase fragments interact in a low-affinity, reversible manner. This reduces the likelihood of false positives and allows the detection of not only

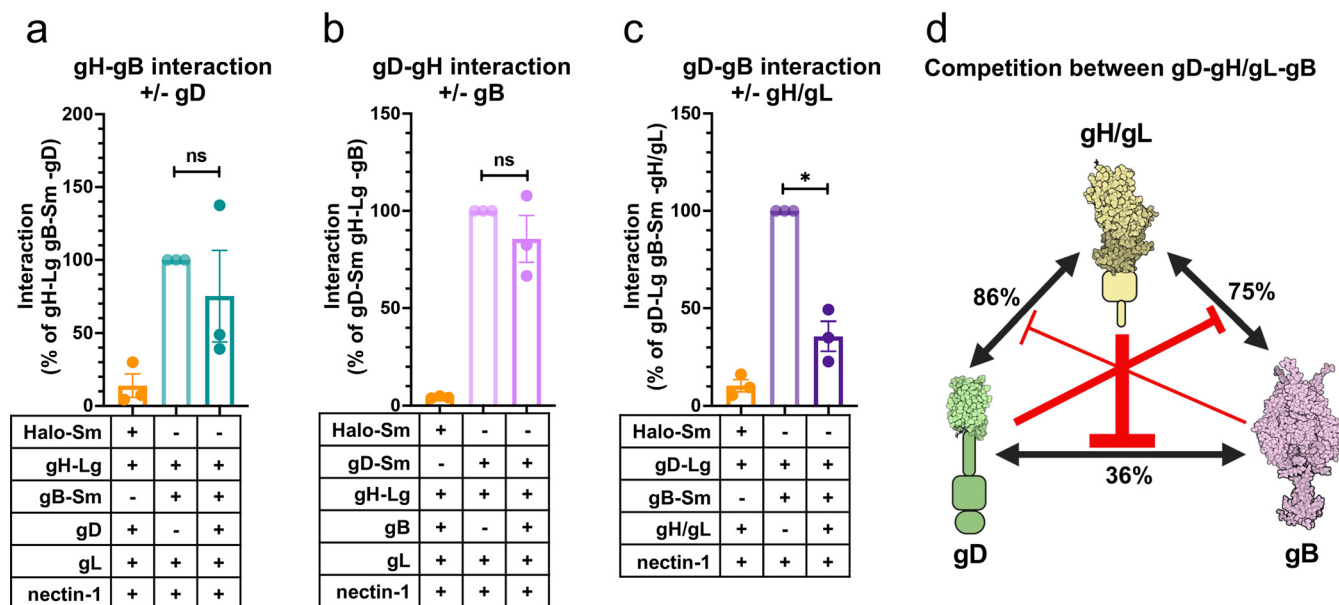


FIG 7 gD, gH/gL, and gB compete with one another for binding. (a) Interaction of gH/gL and gB in the absence versus the presence of gD. (b) Interaction of gD and gH/gL in the absence versus the presence of gB. (c) Interaction of gD and gB in the absence versus the presence of gH/gL. Columns indicate the mean and error bars are the SEM. *, $P < 0.05$. Data represent three biological replicates from independent experiments in all panels. (d) Binding competition model between gD, gH/gL, and gB. The interaction of each pair was decreased in the presence of the third interacting partner, suggesting interaction inhibition by binding competition. The sizes of the red inhibitory arrows are proportional to the degree of inhibition. Values indicate the percentage of the interaction of two interacting partners that remains after inhibition by the presence of the third interacting partner. Created using BioRender.com.

complex association but also dissociation over time. The NanoBiT interaction assay has been used to study transmembrane proteins (61), but as far as we know, this study is the first application of this approach to probing interactions between viral proteins or glycoproteins. The split-luciferase approach is thus a powerful tool that may be broadly applicable across a variety of systems.

We found that pairwise gD-gH/gL, gH/gL-gB, and gD-gB interactions occurred before fusion, remained at a steady level throughout fusion, and were independent of the presence of the receptor nectin-1. As an example, gH/gL interacted with gB in the absence of gD (Fig. 7a) and also interacted with the gB H516P mutant that has been reported to lock gB in the prefusion conformation (12) (Fig. 3f). These findings support the notion that gH/gL-gB interactions occur before fusion (42). The NanoBiT signal for all three pairs, gD-gH/gL, gH/gL-gB, and gD-gB, remained at a steady level upon addition of the receptor-expressing target cells and for the next ~8 h, suggesting that the complexes do not dissociate as gB refolds from the prefusion to the postfusion conformation (Fig. 9b). Therefore, we conclude that the gD-gH/gL, gH/gL-gB, and gD-gB complexes form independently of fusion and are maintained throughout the fusion process.

The detection of gD-gH/gL, gH/gL-gB, and gD-gB interactions using the split-luciferase assay is consistent with previous studies that observed these interactions using split fluorescent proteins (40, 41). However, our observation that the gH/gL-gB interaction occurs before fusion agrees with some reports using split fluorescent proteins (42) but not others (40, 41). We hypothesize that this could be due to a higher sensitivity of the NanoBiT split-luciferase approach used here for detecting interactions (49 and reviewed in reference 44). Alternatively, gD-receptor binding could increase the rate of gH/gL-gB association/dissociation, which could increase the signal due to the irreversibility of the split-fluorescent protein interactions, explaining previous observations (40).

gD-gH/gL and gH/gL-gB interactions involve all HSV-1 gH domains, but the TMD and CT are more important than the ectodomain, and all three domains are required for fusion. Replacing domains of the HSV-1 gH with those of EBV gH or a scrambled sequence revealed that all three domains were involved in gD-gH/gL and gH/gL-gB interactions. For example, when the TMD or CT were the only endogenous

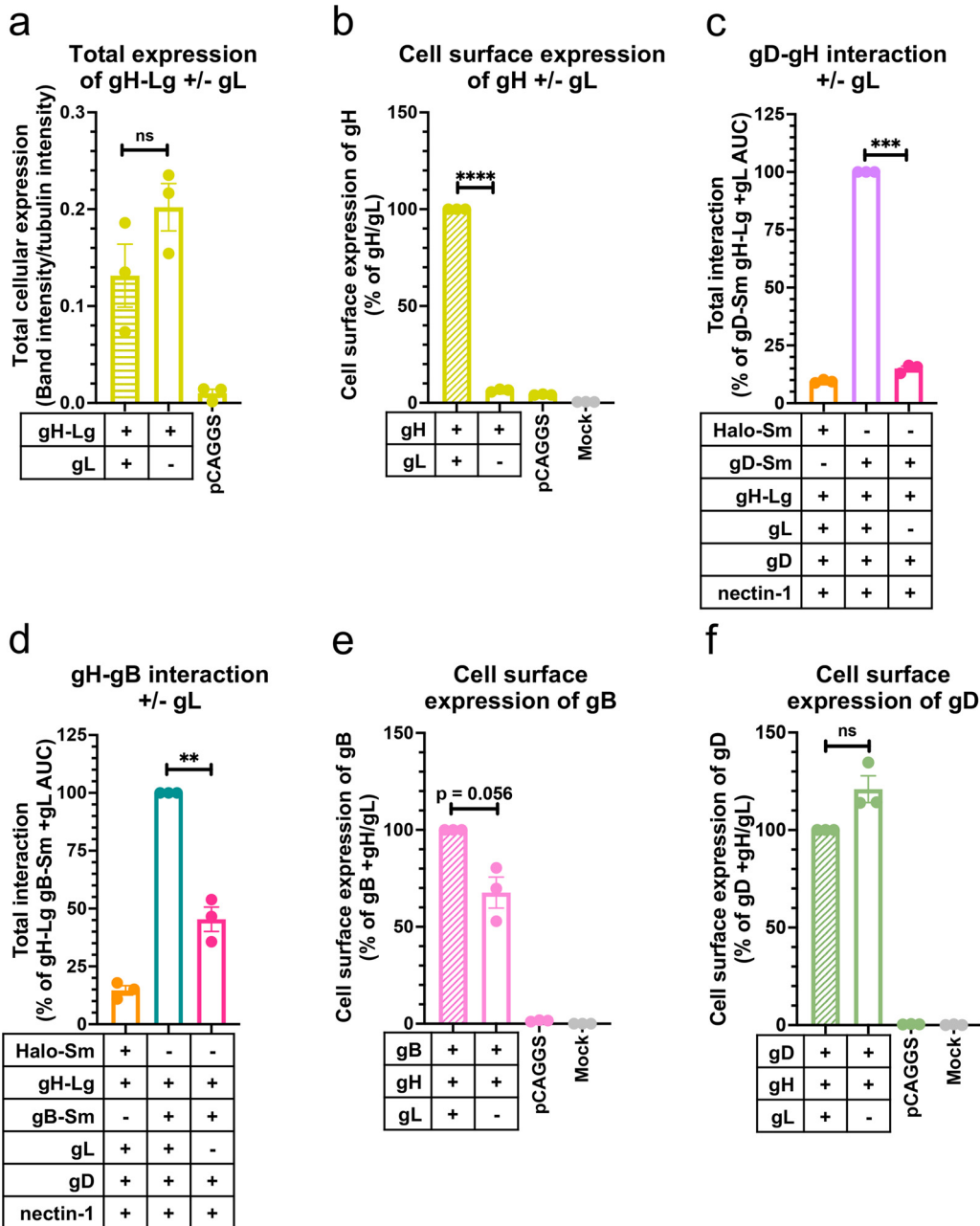


FIG 8 HSV-1 gL is required for gH-gB and gD-gH interactions and for cell surface expression of gH and gB. (a) Total cellular expression of gH-Lg in the presence versus the absence of gL. (b) gH cell surface expression in the presence versus the absence of gL (60, 70) using R137. (c) gD-gH interaction in the presence versus the absence of gL. (d) gH-gB interaction in the presence versus the absence of gL. (e) gB cell surface expression in the presence versus the absence of gL. (f) gD cell surface expression in the presence versus the absence of gL. Columns are the mean. Error bars are the SEM. **, $P < 0.01$; ***, $P < 0.001$; ****, $P < 0.0001$. Data represent three biological replicates from independent experiments in all panels.

HSV-1 gH domains, the chimeric gH could maintain WT-level interactions with HSV-1 gD and gB. However, when the ectodomain was the only endogenous HSV-1 gH domain, interaction with HSV-1 gD and gB decreased ~2-fold. Therefore, gD-gH/gL and gH/gL-gB interactions through their TMDs and CTDs are greater than those through their ectodomains. Whereas previous studies focused mainly on ectodomain interactions (38, 39, 62), our study highlights the previously overlooked yet important contributions of the TMD and CTDs to HSV-1 glycoprotein interactions. Indeed, our recent study proposed a mechanism by which the cytoplasmic tail of gH activates gB through its CTD (63).

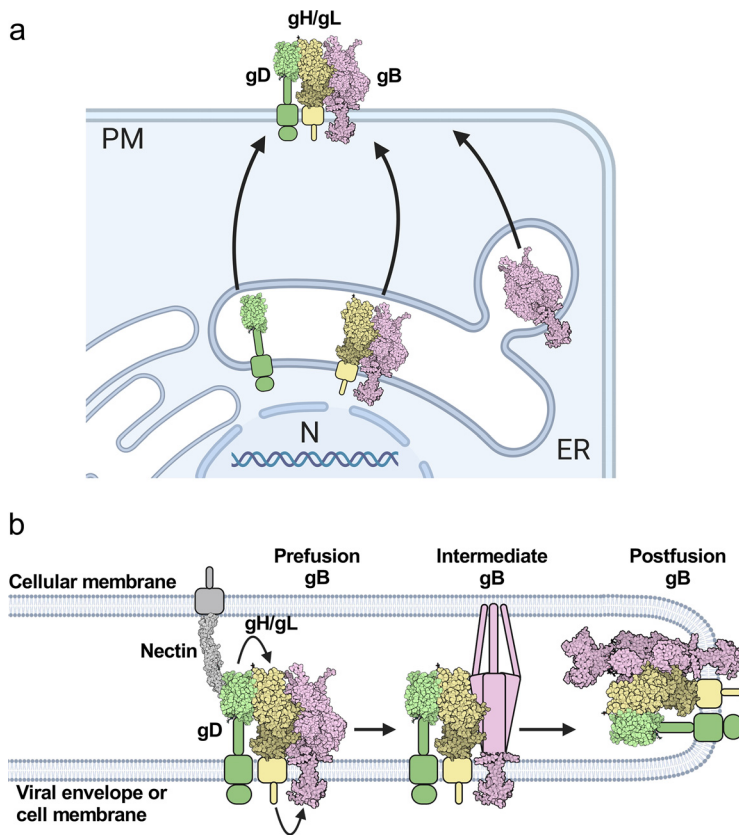


FIG 9 gD-gH/gL-gB trafficking, interaction, and fusion models. (a) Intracellular interactions and trafficking of gD, gH/gL, and gB. gD does not interact with gH in the ER and traffics independently of gH to the plasma membrane. gB interacts with gH in the ER and may traffic with gH/gL to the plasma membrane. Some gB traffics to the plasma membrane without gH/gL. gD, gH/gL, and gB all interact with one another once they leave the ER and compete with one another for binding. gH/gL inhibits binding of the other two binding partners the most, suggesting it binds well to both gD and gB and may position itself between gD and gB in the putative gD-gH/gL-gB complex. gH/gL interacts with gD and gB through all three domains. Cell and glycoprotein sizes are not to scale. (b) New HSV-1 fusion pathway model. gD, gH/gL, and gB are all interacting with each other before fusion. Nectin-1 binds to gD, causing a conformational change (not shown), which activates gH/gL via their ectodomains. gH/gL undergoes a conformational change (not shown) and the gH_{CT} activates the gB_{CTD}. The gB ectodomain refolds and catalyzes membrane fusion. gD, gH/gL, and gB continue to interact. For this model we assume a complex with a 1:1:1 ratio of gD:gH/gL:gB, but the true stoichiometry is unknown.

Surprisingly, when the TMD or CT were the only endogenous HSV-1 gH domains present, the gH/gL-gB interaction was enhanced ~2-fold (Fig. 4f). One possible explanation for this could be a competition for binding of gB to the HSV-1 gH/gL ectodomain by an unknown host protein. Such a competitor would be unable to bind the constructs containing the EBV gH/gL ectodomain, which could explain increased binding of those constructs to HSV-1 gB relative to WT HSV-1 gH/gL. Indeed, integrins have been reported to bind HSV-1 gH/gL (64, 65).

While each of the HSV-1 gH/gL domains, to a certain extent, could maintain interactions with gD and gB, replacing any of the HSV-1 gH/gL domains with those of EBV gH or a scrambled sequence significantly reduced fusion (Fig. 4g). These findings suggest that all three HSV-1 gH/gL domains are required for fusion and that they each perform a specific function in fusion beyond interaction with gD and gB, such as transduction of the triggering signal from gD to gB.

gH/gL blocks gD-gB interactions. We found that the gD-gH/gL, gH/gL-gB, and gD-gB interactions could occur in the absence of the third interacting partner. Moreover, these pairwise interactions were greater when the third partner was absent (Fig. 7a to

c), which suggested that each interacting partner inhibited the interactions of the other two partners. Since all three glycoproteins interact with one another, this inhibitory effect could be due to competition based on shared or overlapping binding sites, allosteric effects, or steric crowding. Interestingly, the inhibitory effect of gD on the gH/gL-gB interaction and gB on the gD-gH/gL interaction was relatively modest and statistically insignificant. In contrast, gH/gL caused a statistically significant, ~3-fold reduction in gD-gB interaction. This suggests that gD and gB preferentially bind to gH/gL rather than to each other, which positions gH/gL in between gD and gB in a putative gD-gH/gL-gB complex and supports the role of gH/gL as the middleman between gD and gB (reviewed in reference 66).

gD and gB differ in their trafficking and interactions with gH/gL. HSV-1 gD, gH/gL, and gB are produced in the ER, traffic to the plasma membrane, and become endocytosed, ending up in vesicles derived from the endosomes or *trans*-Golgi network that serve as virion assembly sites during infection (67, 68). Alphaherpesvirus glycoprotein traffic from the ER to the plasma membrane is thought to occur by the exocytic pathway (69), but whether HSV-1 gD, gH/gL, and gB interact during this process is unknown. Once at the plasma membrane, HSV-1 gB can endocytose independently of other viral glycoproteins to reach the virion assembly site, whereas gH/gL and gD require colocalization—and likely interaction—with other glycoproteins such as gM because they lack an endocytic signal (68).

Given the extensive interactions between gD, gH/gL, and gB that we observed in this study, we asked where in the cell they interact and whether these proteins cotraffic to the cell surface. By taking advantage of the inability of gH to leave the ER without gL, we found that in the absence of gL, gD-gH interactions in the ER were minimal, whereas gH-gB interactions in the ER were about 50% of the level of overall gH/gL-gB interactions (Fig. 8c and d). This suggests that gB interacts with gH to a far greater extent in the ER than gD does. In addition, we found that when gH was expressed without gL, gD cell surface expression was unaffected, while gB cell surface expression was reduced. This further supports the hypothesis that gD does not interact with gH in the ER to an appreciable degree because gD is able to leave the ER and traffic to the cell surface unimpeded. In contrast, roughly a third of gB molecules appear to be held back from trafficking to the cell surface due to interactions with gH in the ER. Therefore, we propose that a portion of gH/gL and gB interact in the ER and traffic together to the cell surface in addition to some gB that traffics independently, whereas gD traffics to the cell surface independently and then joins the gH/gL-gB complex on the cell surface (Fig. 9a).

Both gD and gB interact with gH/gL through their ectodomains, TMDs, and CTDs, so it is interesting that gB but not gD interacted with gH in the ER. How is gD able to bind to gH/gL on the cell surface but avoid binding to gH in the ER? It is possible that the gD-gH interaction is more dynamic than the gH-gB interaction, with more frequent dissociation, allowing gD to gradually escape the ER without gH/gL. Another possibility is that the conformation of gH is different in the absence of gL than when it is complexed with gL, which has been suggested in several studies (59, 70, 71), causing decreased gD-gH interaction relative to gD-gH/gL interactions.

New HSV-1 fusion pathway model. Collectively, we postulate that gD, gH/gL, and gB form a gD-gH/gL-gB complex that exists at a steady level, with gH/gL positioned in between gD and gB. A preassembled gD-gH/gL-gB complex in this orientation would enable efficient transmission of an activating signal from gD-receptor interaction to gH/gL to gB to trigger its fusogenic refolding (Fig. 9b). We propose that this signal transduction occurs by the following conformational cascade model. Upon receptor binding to HSV-1 gD, gD undergoes a conformational change (72) that activates the already bound gH/gL ectodomain. This causes a conformational change in the gH/gL ectodomain (38, 47) that is transmitted through the gH TMD and activates the gH CT to alter its interaction with the gB CTD (15, 63, 73). Ultimately, this triggers gB to refold and cause fusion (Fig. 9b) (15). Hence, if any of the HSV-1 gH domains are replaced, the signaling sequence from receptor to gB is disrupted and fusion cannot occur.

Open questions. Here, we identified steady gD-gH/gL, gH/gL-gB, and gD-gB interactions, suggesting that pairs of these interacting partners exist in complexes with one another. However, it is still undetermined whether these pairs exist independently or whether they form the gD-gH/gL-gB complex. Our fusion pathway model (Fig. 9b) favors the latter possibility, which would position the glycoproteins ideally for rapid signal transduction upon receptor binding. It is yet unclear how these complexes change during fusion. The steady interactions observed here for each interaction pair suggest that the complexes do not associate or dissociate during fusion but may, instead, change their conformation to fuse membranes. Furthermore, it is yet unclear how these glycoproteins interact on the virions. How glycoproteins are distributed on the HSV-1 surface and how they interact before and throughout the fusion process are important questions that beg in-depth investigation.

Our data support a model in which gD, gH/gL, and gB interact throughout the fusion process and that their complexes are functionally important. We also hypothesize that these complexes have important roles in membrane fusion. Nonetheless, we cannot yet rule out the possibility that the function of these complexes is something other than membrane fusion. One limitation of our study is that we do not know what fraction of the glycoproteins form complexes or whether fusion is mediated by gB within a glycoprotein complex rather than by free gB that is triggered by a transient interaction with gH/gL. However, most interaction assays, including coimmunoprecipitation, suffer from this limitation. Future single-molecule tracking experiments will be needed to resolve this question.

MATERIALS AND METHODS

Cells and plasmids. CHO cells (74) were gifts from J. M. Coffin and were grown in Ham's F-12 medium with 10% fetal bovine serum (FBS), 100 IU penicillin, and 100 μ g/mL streptomycin at 37°C and 5% CO₂, except when noted otherwise. Plasmids pPEP98, pPEP99, pPEP100, and pPEP101 carry the full-length HSV-1 (strain KOS) gB, gD, gH, and gL genes, respectively, in a pCAGGS vector. These plasmids were gifts from P. G. Spear (Northwestern University) (75). Plasmids RLuc8₁₋₇ and RLuc8₈₋₁₁ (encoding the *Renilla* split luciferase genes) and pBG38 (carrying the nectin-1 gene) were gifts from G. H. Cohen and R. J. Eisenberg (University of Pennsylvania) (51, 76). Plasmid pJLS11 (gB868) was generated previously (55). Plasmids for the NanoBiT interaction assay, including PRKACA-Sm and PRKAR2A-Lg positive-control plasmids, the Halo-Sm negative-control plasmid, and Sm- and Lg-BiT plasmids for tagging proteins of interest were purchased from Promega (Madison, WI) (49). All plasmids from Promega contained an HSV-TK promoter. Plasmids p85 and p25 carry the full-length EBV gH and EBV gL genes in a pCAGGS vector, respectively, and were gifts from R. M. Longnecker (Northwestern University).

Cloning. The cloning strategies and primers used to generate the constructs used in this paper are included in Text S1 and Table S1 in the supplemental material.

Western blotting. Total cellular expression of NanoBiT constructs was tested using Western blotting. CHO cells were seeded at 2.5×10^5 cells per well in 6-well plates. The next day, DNA constructs of interest were transfected. On day 3, cells were treated with RIPA buffer and a protease inhibitor and collected and spun down. The supernatants were mixed with SDS-PAGE loading dye and heated for 5 min at 95°C. Samples were separated by electrophoresis, transferred onto nitrocellulose membranes, and blocked. Strips of membranes were incubated with the appropriate primary antibody overnight at 4°C. On day 4, membranes were incubated with fluorescent secondary antibodies for 1 h at room temperature. Membranes were imaged using a LI-COR Odyssey imager. More detailed methods are included in Text S1 in the supplemental material.

Flow cytometry. Cell surface expression of gB, gH/gL, and gD constructs were evaluated using flow cytometry. CHO cells were seeded at 2.5×10^5 cells per well in 6-well plates. The next day, each well was transfected with DNA constructs of interest. On day 3, cells were collected and incubated for 1 h on ice with appropriate primary antibodies. Cells were washed, incubated for 1 h on ice in the dark with secondary antibodies, and washed again. The fluorescence of the cells was determined by flow cytometry. More detailed methods are included in Text S1 in the supplemental material.

NanoBiT interaction assay. Interactions between glycoproteins were measured using the NanoBiT interaction assay (49). CHO cells were seeded into 6-well plates at 2.5×10^5 cells per well for effector cells and 6-well plates at 2×10^5 cells per well for target cells. The next day, effector cells were transfected with DNA of the two interacting partners and any remaining HSV-1 proteins required for fusion. Target cells were transfected with nectin-1 (pBG38) or pCAGGS; 4 h later, the effector cells were collected and seeded into 3 wells per condition in a 96-well plate. On day 3, the medium of the effector cells was replaced with 40 μ L per well of fusion medium (Ham's F12 with 10% FBS, penicillin/streptomycin, 50 mM HEPES) with 1:50 Endurazine luciferase substrate (Promega) added. Cells were placed in a BioTek plate reader. Luminescence measurements were taken every 2 min for 1 h at 37°C. Meanwhile, target cells were collected and resuspended in fusion medium. Then, 40 μ L of target cells was added to each well of effector cells. Luminescence measurements were taken every 2 min for 7.5 or 8 h. More detailed methods are included in the Text S1 in the supplemental material.

Cell-cell fusion assay. Cell-cell fusion of gB, gH/gL, and gD constructs was tested using a split-luciferase assay (51). CHO cells were seeded into 3 wells per condition in a 96-well plate at 5×10^4 cells per well for effector cells and 6-well plates at 2×10^5 cells per well for target cells. The next day, effector cells were transfected with DNA of constructs of interest and part of a split luciferase (Rluc8₁₋₇). Each well of target cells was transfected with the complementary part of the split luciferase (Rluc8₈₋₁₁) and nectin-1. On day 3, the medium of the effector cells was replaced with 40 μ L per well of fusion medium with 1:500 EnduRen luciferase substrate (Promega) added. Cells were incubated for 1 h at 37°C. In the meantime, target cells were collected and resuspended in fusion medium. Then, 40 μ L of target cells was added to each well of effector cells. The plate was immediately placed in a BioTek plate reader. Luminescence measurements were taken every 2 min for 2 h followed by measurements every hour for 6 h. More detailed methods are included in Text S1 in the supplemental material.

Statistics. Statistical analysis was done for each experiment using GraphPad Prism 9 software. An unpaired *t* test with Welch's correction was used to compare conditions to each other as shown.

SUPPLEMENTAL MATERIAL

Supplemental material is available online only.

TEXT S1, DOCX file, 0.02 MB.

TABLE S1, DOCX file, 0.03 MB

ACKNOWLEDGMENTS

We thank Erin Sanders for help with cloning, flow cytometry, and fusion experiments. We thank Stephen Kwok and Allen Parmelee at the Tufts Flow Cytometry Core and Adam Hilterbrand for flow cytometry training. We thank Bing Dai for advice regarding Western blotting. We thank Scott Messenger (Promega) for technical advice regarding the NanoBiT interaction assay. We thank Roselyn J. Eisenberg and Gary H. Cohen (University of Pennsylvania) for the gift of plasmids and antibodies. We thank Richard Longnecker (Northwestern University) for the gift of plasmids and antibodies. We thank Patricia Spear (Northwestern University) for the gift of plasmids. We thank Andrew McGuire (Fred Hutchinson Cancer Research Center) for the gift of antibodies. We thank John Coffin, Marta Gaglia, Karl Munger, and Ellen White for helpful discussions.

Research reported in this publication was supported by the National Institutes of Health under award numbers T32GM731042 (Z.P.), T32GM731043 (Z.P.), F30AI161795 (Z.P.), and R01AI164698 (E.E.H.) and by a Faculty Scholar grant 55108533 from Howard Hughes Medical Institute (E.E.H.). The content is solely the responsibility of the authors and does not necessarily represent the official views of the National Institutes of Health. We dedicate this publication to the memory of Roselyn J. Eisenberg (University of Pennsylvania)."

Z.P. designed the experiments, cloned the constructs, conducted the experiments, analyzed the data, generated hypotheses, generated models, and wrote the manuscript. A.R.V. cloned constructs, conducted experiments, analyzed the data, and generated hypotheses. E.E.H. designed experiments, analyzed the data, generated hypotheses, generated models, and wrote the manuscript.

REFERENCES

- Harrison SC. 2008. Viral membrane fusion. *Nat Struct Mol Biol* 15:690–698. <https://doi.org/10.1038/nmsb.1456>.
- Connolly SA, Jardetzky TS, Longnecker R. 2021. The structural basis of herpesvirus entry. *Nat Rev Microbiol* 19:110–121. <https://doi.org/10.1038/s41579-020-00448-w>.
- Cohen JL. 2020. Herpesvirus latency. *J Clin Invest* 130:3361–3369. <https://doi.org/10.1172/JCI136225>.
- Renner DW, Szpara ML. 2018. Impacts of genome-wide analyses on our understanding of human herpesvirus diversity and evolution. *J Virol* 92:e00908-17. <https://doi.org/10.1128/JVI.00908-17>.
- Looker KJ, Magaret AS, May MT, Turner KM, Vickerman P, Gottlieb SL, Newman LM. 2015. Global and regional estimates of prevalent and incident herpes simplex virus type 1 infections in 2012. *PLoS One* 10:e0140765. <https://doi.org/10.1371/journal.pone.0140765>.
- Arduino PG, Porter SR. 2008. Herpes simplex virus type 1 infection: overview on relevant clinico-pathological features. *J Oral Pathol Med* 37:107–121. <https://doi.org/10.1111/j.1600-0714.2007.00586.x>.
- Steiner I, Benninger F. 2013. Update on herpes virus infections of the nervous system. *Curr Neurol Neurosci Rep* 13:414. <https://doi.org/10.1007/s11910-013-0414-8>.
- Sauerbrei A, Wutzler P. 2007. Herpes simplex and varicella-zoster virus infections during pregnancy: current concepts of prevention, diagnosis and therapy. part 1: herpes simplex virus infections. *Med Microbiol Immunol* 196:89–94. <https://doi.org/10.1007/s00430-006-0031-0>.
- Whitley R, Kimberlin DW, Prober CG. 2007. Pathogenesis and disease. *In* Arvin A, Campadelli-Fiume G, Mocarski E, Moore PS, Roizman B, Whitley R, Yamanishi K (ed), *Human herpesviruses: biology, therapy, and immunoprophylaxis*. Cambridge University Press, Cambridge, UK.
- Poole CL, James SH. 2018. Antiviral therapies for herpesviruses: current agents and new directions. *Clin Ther* 40:1282–1298. <https://doi.org/10.1016/j.clinthera.2018.07.006>.
- Bernstein DI, Pullum DA, Cardin RD, Bravo FJ, Dixon DA, Kousoulas KG. 2019. The HSV-1 live attenuated VC2 vaccine provides protection against HSV-2 genital infection in the guinea pig model of genital herpes. *Vaccine* 37:61–68. <https://doi.org/10.1016/j.vaccine.2018.11.042>.

12. Vollmer B, Prazak V, Vasishtan D, Jefferys EE, Hernandez-Duran A, Vallbracht M, Klupp BG, Mettenleiter TC, Backovic M, Rey FA, Topf M, Grunewald K. 2020. The prefusion structure of herpes simplex virus glycoprotein B. *Sci Adv* 6:eabc1726. <https://doi.org/10.1126/sciadv.abc1726>.
13. Liu Y, Heim KP, Che Y, Chi X, Qiu X, Han S, Dormitzer PR, Yang X. 2021. Prefusion structure of human cytomegalovirus glycoprotein B and structural basis for membrane fusion. *Sci Adv* 7:eabf3178. <https://doi.org/10.1126/sciadv.abf3178>.
14. Heldwein EE, Lou H, Bender FC, Cohen GH, Eisenberg RJ, Harrison SC. 2006. Crystal structure of glycoprotein B from herpes simplex virus 1. *Science* 313:217–220. <https://doi.org/10.1126/science.1126548>.
15. Cooper RS, Georgieva ER, Borbat PP, Freed JH, Heldwein EE. 2018. Structural basis for membrane anchoring and fusion regulation of the herpes simplex virus fusing gB. *Nat Struct Mol Biol* 25:416–424. <https://doi.org/10.1038/s41594-018-0060-6>.
16. Burke HG, Heldwein EE. 2015. Crystal structure of the human cytomegalovirus glycoprotein B. *PLoS Pathog* 11:e1005227. <https://doi.org/10.1371/journal.ppat.1005227>.
17. Vallbracht M, Brun D, Tassinari M, Vaney MC, Pehau-Arnaudet G, Guardado-Calvo P, Haouz A, Klupp BG, Mettenleiter TC, Rey FA, Backovic M. 2018. Structure-function dissection of pseudorabies virus glycoprotein B fusion loops. *J Virol* 92:e01203-17. <https://doi.org/10.1128/JVI.01203-17>.
18. Backovic M, Longnecker R, Jardetzky TS. 2009. Structure of a trimeric variant of the Epstein-Barr virus glycoprotein B. *Proc Natl Acad Sci U S A* 106:2880–2885. <https://doi.org/10.1073/pnas.0810530106>.
19. Vallbracht M, Lotzsch H, Klupp BG, Fuchs W, Vollmer B, Grunewald K, Backovic M, Rey FA, Mettenleiter TC. 2021. In vitro viral evolution identifies a critical residue in the alphaherpesvirus fusion glycoprotein B ectodomain that controls gH/gL-independent entry. *mBio* 12:e00557-21. <https://doi.org/10.1128/mBio.00557-21>.
20. McShane MP, Longnecker R. 2004. Cell-surface expression of a mutated Epstein-Barr virus glycoprotein B allows fusion independent of other viral proteins. *Proc Natl Acad Sci U S A* 101:17474–17479. <https://doi.org/10.1073/pnas.0404535101>.
21. Chen J, Zhang X, Schaller S, Jardetzky TS, Longnecker R. 2019. Ephrin receptor A4 is a new Kaposi's sarcoma-associated herpesvirus entry receptor. *mBio* 10:e02892-18. <https://doi.org/10.1128/mBio.02892-18>.
22. Hahn AS, Kaufmann JK, Wies E, Naschberger E, Panteleev-Ivlev J, Schmidt K, Holzer A, Schmidt M, Chen J, König S, Ensser A, Myoung J, Brockmeyer NH, Stürzl M, Fleckenstein B, Neipel F. 2012. The ephrin receptor tyrosine kinase A2 is a cellular receptor for Kaposi's sarcoma-associated herpesvirus. *Nat Med* 18:961–966. <https://doi.org/10.1038/nm.2805>.
23. Yang E, Arvin AM, Oliver SL. 2016. Role for the αV integrin subunit in varicella-zoster virus-mediated fusion and infection. *J Virol* 90:7567–7578. <https://doi.org/10.1128/JVI.00792-16>.
24. Chen J, Sathiyamoorthy K, Zhang X, Schaller S, Perez White BE, Jardetzky TS, Longnecker R. 2018. Ephrin receptor A2 is a functional entry receptor for Epstein-Barr virus. *Nat Microbiol* 3:172–180. <https://doi.org/10.1038/s41564-017-0081-7>.
25. Gonzalez-Del Pino GL, Heldwein EE. 2022. Well put together—a guide to accessorizing with the herpesvirus gH/gL complexes. *Viruses* 14:296. <https://doi.org/10.3390/v14020296>.
26. Carfi A, Willis SH, Whitbeck JC, Krummenacher C, Cohen GH, Eisenberg RJ, Wiley DC. 2001. Herpes simplex virus glycoprotein D bound to the human receptor HveA. *Mol Cell* 8:169–179. [https://doi.org/10.1016/S1097-2765\(01\)00298-2](https://doi.org/10.1016/S1097-2765(01)00298-2).
27. Di Giovine P, Settembre EC, Bhargava AK, Luftig MA, Lou H, Cohen GH, Eisenberg RJ, Krummenacher C, Carfi A. 2011. Structure of herpes simplex virus glycoprotein D bound to the human receptor nectin-1. *PLoS Pathog* 7:e1002277. <https://doi.org/10.1371/journal.ppat.1002277>.
28. Spear PG. 2004. Herpes simplex virus: receptors and ligands for cell entry. *Cell Microbiol* 6:401–410. <https://doi.org/10.1111/j.1462-5822.2004.00389.x>.
29. Martinez-Martin N, Marcandalli J, Huang CS, Arthur CP, Perotti M, Foglierini M, Ho H, Dosey AM, Shriver S, Payandeh J, Leitner A, Lanzavecchia A, Perez L, Ciferri C. 2018. An unbiased screen for human cytomegalovirus identifies neuropilin-2 as a central viral receptor. *Cell* 174:1158–1171.e19. <https://doi.org/10.1016/j.cell.2018.06.028>.
30. Kabanova A, Marcandalli J, Zhou T, Bianchi S, Baxa U, Tsybovsky Y, Lillier D, Silacci-Fregni C, Foglierini M, Fernandez-Rodriguez BM, Druz A, Zhang B, Geiger R, Pagani M, Sallusto F, Kwong PD, Corti D, Lanzavecchia A, Perez L. 2016. Platelet-derived growth factor- α receptor is the cellular receptor for human cytomegalovirus gHgLgO trimer. *Nat Microbiol* 1:16082. <https://doi.org/10.1038/nmicrobiol.2016.82>.
31. Wu Y, Prager A, Boos S, Resch M, Brizic I, Mach M, Wildner S, Scrivano L, Adler B. 2017. Human cytomegalovirus glycoprotein complex gH/gL/gO uses PDGFR- α as a key for entry. *PLoS Pathog* 13:e1006281. <https://doi.org/10.1371/journal.ppat.1006281>.
32. Mullen MM, Haan KM, Longnecker R, Jardetzky TS. 2002. Structure of the Epstein-Barr virus gp42 protein bound to the MHC class II receptor HLA-DR1. *Mol Cell* 9:375–385. [https://doi.org/10.1016/S1097-2765\(02\)00465-3](https://doi.org/10.1016/S1097-2765(02)00465-3).
33. Sathiyamoorthy K, Hu YX, Möhl BS, Chen J, Longnecker R, Jardetzky TS. 2016. Structural basis for Epstein-Barr virus host cell tropism mediated by gp42 and gHgL entry glycoproteins. *Nat Commun* 7:13557. <https://doi.org/10.1038/ncomms13557>.
34. Chandramouli S, Malito E, Nguyen T, Luisi K, Donnarumma D, Xing Y, Norais N, Yu D, Carfi A. 2017. Structural basis for potent antibody-mediated neutralization of human cytomegalovirus. *Sci Immunol* 2:eaan1457. <https://doi.org/10.1126/sciimmunol.aan1457>.
35. Ciferri C, Chandramouli S, Leitner A, Donnarumma D, Cianfrocco MA, Gerrein R, Friedrich K, Aggarwal Y, Palladino G, Aebersold R, Norais N, Settembre EC, Carfi A. 2015. Antigenic characterization of the HCMV gH/gL/gO and pentamer cell entry complexes reveals binding sites for potentially neutralizing human antibodies. *PLoS Pathog* 11:e1005230. <https://doi.org/10.1371/journal.ppat.1005230>.
36. Vanarsdall AL, Howard PW, Wisner TW, Johnson DC. 2016. Human cytomegalovirus gH/gL forms a stable complex with the fusion protein gB in virions. *PLoS Pathog* 12:e1005564. <https://doi.org/10.1371/journal.ppat.1005564>.
37. Si Z, Zhang J, Shivakoti S, Atanasov I, Tao CL, Hui WH, Zhou K, Yu X, Li W, Luo M, Bi GQ, Zhou ZH. 2018. Different functional states of fusion protein gB revealed on human cytomegalovirus by cryo electron tomography with Volta phase plate. *PLoS Pathog* 14:e1007452. <https://doi.org/10.1371/journal.ppat.1007452>.
38. Cairns TM, Atanasiu D, Saw WT, Lou H, Whitbeck JC, Ditto NT, Bruun B, Browne H, Bennett L, Wu C, Krummenacher C, Brooks BD, Eisenberg RJ, Cohen GH. 2020. Localization of the interaction site of herpes simplex virus glycoprotein D (gD) on the membrane fusion regulator, gH/gL. *J Virol* 94:e00983-20. <https://doi.org/10.1128/JVI.00983-20>.
39. Cairns TM, Ditto NT, Atanasiu D, Lou H, Brooks BD, Saw WT, Eisenberg RJ, Cohen GH. 2019. Surface plasmon resonance reveals direct binding of herpes simplex virus glycoproteins gH/gL to gD and locates a gH/gL binding site on gD. *J Virol* 93:e00289-19. <https://doi.org/10.1128/JVI.00289-19>.
40. Atanasiu D, Whitbeck JC, Cairns TM, Reilly B, Cohen GH, Eisenberg RJ. 2007. Bimolecular complementation reveals that glycoproteins gB and gH/gL of herpes simplex virus interact with each other during cell fusion. *Proc Natl Acad Sci U S A* 104:18718–18723. <https://doi.org/10.1073/pnas.0707452104>.
41. Avitabile E, Forghieri C, Campadelli-Fiume G. 2007. Complexes between herpes simplex virus glycoproteins gD, gB, and gH detected in cells by complementation of split enhanced green fluorescent protein. *J Virol* 81:11532–11537. <https://doi.org/10.1128/JVI.01343-07>.
42. Avitabile E, Forghieri C, Campadelli-Fiume G. 2009. Cross talk among the glycoproteins involved in herpes simplex virus entry and fusion: the interaction between gB and gH/gL does not necessarily require gD. *J Virol* 83:10752–10760. <https://doi.org/10.1128/JVI.01287-09>.
43. Connolly SA, Leser GP, Jardetzky TS, Lamb RA. 2009. Bimolecular complementation of paramyxovirus fusion and hemagglutinin-neuraminidase proteins enhances fusion: implications for the mechanism of fusion triggering. *J Virol* 83:10857–10868. <https://doi.org/10.1128/JVI.01191-09>.
44. Romei MG, Boxer SG. 2019. Split green fluorescent proteins: scope, limitations, and outlook. *Annu Rev Biophys* 48:19–44. <https://doi.org/10.1146/annurev-biophys-051013-022846>.
45. Atanasiu D, Saw WT, Cohen GH, Eisenberg RJ. 2010. Cascade of events governing cell-cell fusion induced by herpes simplex virus glycoproteins gD, gH/gL, and gB. *J Virol* 84:12292–12299. <https://doi.org/10.1128/JVI.01700-10>.
46. Cocchi F, Fusco D, Menotti L, Gianni T, Eisenberg RJ, Cohen GH, Campadelli-Fiume G. 2004. The soluble ectodomain of herpes simplex virus gD contains a membrane-proximal pro-fusion domain and suffices to mediate virus entry. *Proc Natl Acad Sci U S A* 101:7445–7450. <https://doi.org/10.1073/pnas.0401883101>.
47. Atanasiu D, Cairns TM, Whitbeck JC, Saw WT, Rao S, Eisenberg RJ, Cohen GH. 2013. Regulation of herpes simplex virus gB-induced cell-cell fusion by mutant forms of gH/gL in the absence of gD and cellular receptors. *mBio* 4:e00046-13. <https://doi.org/10.1128/mBio.00046-13>.
48. Heldwein EE, Krummenacher C. 2008. Entry of herpesviruses into mammalian cells. *Cell Mol Life Sci* 65:1653–1668. <https://doi.org/10.1007/s00018-008-7570-z>.
49. Dixon AS, Schwinn MK, Hall MP, Zimmerman K, Otto P, Lubben TH, Butler BL, Binkowski BF, Machleidt T, Kirkland TA, Wood MG, Eggers CT, Encell

- LP, Wood KV. 2016. NanoLuc complementation reporter optimized for accurate measurement of protein interactions in cells. *ACS Chem Biol* 11: 400–408. <https://doi.org/10.1021/acschembio.5b00753>.
50. Promega. 2021. NanoBIT protein:protein interaction system technical manual. www.promega.com. Accessed 6 March 2022.
51. Saw WT, Matsuda Z, Eisenberg RJ, Cohen GH, Atanasiu D. 2015. Using a split luciferase assay (SLA) to measure the kinetics of cell-cell fusion mediated by herpes simplex virus glycoproteins. *Methods* 90:68–75. <https://doi.org/10.1016/j.ymeth.2015.05.021>.
52. England CG, Luo H, Cai W. 2015. HaloTag technology: a versatile platform for biomedical applications. *Bioconjug Chem* 26:975–986. <https://doi.org/10.1021/acs.bioconjchem.5b00191>.
53. Lee SK, Compton T, Longnecker R. 1997. Failure to complement infectivity of EBV and HSV-1 glycoprotein B (gB) deletion mutants with gBs from different human herpesvirus subfamilies. *Virology* 237:170–181. <https://doi.org/10.1006/viro.1997.8765>.
54. Promega. 2018. Nano-Glo Endurazine and Vivazine live cell substrates technical manual. https://www.promega.com/-/media/files/resources/protocols/technical-manuals/500/nano-glo-endurazine-and-vivazine-live-cell-substrates-technical-manual.pdf?rev=6bcfcbefee4f4cad8a6a14a6697ae39b&sc_lang=en
55. Silverman JL, Greene NG, King DS, Heldwein EE. 2012. Membrane requirement for folding of the herpes simplex virus 1 gB cytodomain suggests a unique mechanism of fusion regulation. *J Virol* 86:8171–8184. <https://doi.org/10.1128/JVI.00932-12>.
56. Zeev-Ben-Mordehai T, Vasishtan D, Siebert CA, Whittle C, Grünwald K. 2014. Extracellular vesicles: a platform for the structure determination of membrane proteins by cryo-EM. *Structure* 22:1687–1692. <https://doi.org/10.1016/j.str.2014.09.005>.
57. Zeev-Ben-Mordehai T, Vasishtan D, Hernandez Duran A, Vollmer B, White P, Prasad Pandurangan A, Siebert CA, Topf M, Grunewald K. 2016. Two distinct trimeric conformations of natively membrane-anchored full-length herpes simplex virus 1 glycoprotein B. *Proc Natl Acad Sci U S A* 113:4176–4181. <https://doi.org/10.1073/pnas.1523234113>.
58. Maurer UE, Zeev-Ben-Mordehai T, Pandurangan AP, Cairns TM, Hannah BP, Whitbeck JC, Eisenberg RJ, Cohen GH, Topf M, Huisken JT, Grunewald K. 2013. The structure of herpesvirus fusion glycoprotein B-bilayer complex reveals the protein-membrane and lateral protein-protein interaction. *Structure* 21:1396–1405. <https://doi.org/10.1016/j.str.2013.05.018>.
59. Hutchinson L, Browne H, Wargent V, Davis-Poynter N, Primorac S, Goldsmith K, Minson AC, Johnson DC. 1992. A novel herpes simplex virus glycoprotein, gL, forms a complex with glycoprotein H (gH) and affects normal folding and surface expression of gH. *J Virol* 66:2240–2250. <https://doi.org/10.1128/JVI.66.4.2240-2250.1992>.
60. Cairns TM, Friedman LS, Lou H, Whitbeck JC, Shaner MS, Cohen GH, Eisenberg RJ. 2007. N-terminal mutants of herpes simplex virus type 2 gH are transported without gL but require gL for function. *J Virol* 81: 5102–5111. <https://doi.org/10.1128/JVI.00097-07>.
61. Peach CJ, Kilpatrick LE, Woolard J, Hill SJ. 2021. Use of NanoBIT and NanoBRET to monitor fluorescent VEGF-A binding kinetics to VEGFR2/NRP1 heteromeric complexes in living cells. *Br J Pharmacol* 178:2393–2411. <https://doi.org/10.1111/bph.15426>.
62. Atanasiu D, Saw WT, Cairns TM, Eisenberg RJ, Cohen GH. 2021. Using split luciferase assay and anti-Herpes Simplex Virus glycoprotein monoclonal antibodies to predict a functional binding site between gD and gH/gL. *J Virol* 95:e00053-21. <https://doi.org/10.1128/JVI.00053-21>.
63. Pataki Z, Sanders EK, Heldwein EE. 2022. A surface pocket in the cytoplasmic domain of the herpes simplex virus fusogen gB controls membrane fusion. *PLoS Pathog* 18:e1010435. <https://doi.org/10.1371/journal.ppat.1010435>.
64. Gianni T, Massaro R, Campadelli-Fiume G. 2015. Dissociation of HSV gL from gH by alphavbeta6- or alphavbeta8-integrin promotes gH activation and virus entry. *Proc Natl Acad Sci U S A* 112:E3901–E3910. <https://doi.org/10.1073/pnas.1506846112>.
65. Gianni T, Salvioli S, Chesnokova LS, Hutt-Fletcher LM, Campadelli-Fiume G. 2013. $\alpha v\beta 6$ - and $\alpha v\beta 8$ -integrins serve as interchangeable receptors for HSV gH/gL to promote endocytosis and activation of membrane fusion. *PLoS Pathog* 9:e1003806. <https://doi.org/10.1371/journal.ppat.1003806>.
66. Stampfer SD, Heldwein EE. 2013. Stuck in the middle: structural insights into the role of the gH/gL heterodimer in herpesvirus entry. *Curr Opin Virol* 3:13–19. <https://doi.org/10.1016/j.coviro.2012.10.005>.
67. Hollinshead M, Johns HL, Sayers CL, Gonzalez-Lopez C, Smith GL, Elliott G. 2012. Endocytic tubules regulated by Rab GTPases 5 and 11 are used for envelopment of herpes simplex virus. *EMBO J* 31:4204–4220. <https://doi.org/10.1038/emboj.2012.262>.
68. Albecka A, Laine RF, Janssen AF, Kaminski CF, Crump CM. 2016. HSV-1 glycoproteins are delivered to virus assembly sites through dynamin-dependent endocytosis. *Traffic* 17:21–39. <https://doi.org/10.1111/tra.12340>.
69. Hogue IB, Scherer J, Enquist LW. 2016. Exocytosis of alphaherpesvirus virions, light particles, and glycoproteins uses constitutive secretory mechanisms. *mBio* 7:e00820-16. <https://doi.org/10.1128/mBio.00820-16>.
70. Roberts SR, Ponce de Leon M, Cohen GH, Eisenberg RJ. 1991. Analysis of the intracellular maturation of the herpes simplex virus type 1 glycoprotein gH in infected and transfected cells. *Virology* 184:609–624. [https://doi.org/10.1016/0042-6822\(91\)90431-a](https://doi.org/10.1016/0042-6822(91)90431-a).
71. Gompels UA, Minson AC. 1989. Antigenic properties and cellular localization of herpes simplex virus glycoprotein H synthesized in a mammalian cell expression system. *J Virol* 63:4744–4755. <https://doi.org/10.1128/JVI.63.11.4744-4755.1989>.
72. Krummenacher C, Supekar VM, Whitbeck JC, Lazear E, Connolly SA, Eisenberg RJ, Cohen GH, Wiley DC, Carfi A. 2005. Structure of unliganded HSV gD reveals a mechanism for receptor-mediated activation of virus entry. *EMBO J* 24:4144–4153. <https://doi.org/10.1038/sj.emboj.7600875>.
73. Rogalin HB, Heldwein EE. 2015. Interplay between the herpes simplex virus 1 gB cytodomain and the gH cytotail during cell-cell fusion. *J Virol* 89: 12262–12272. <https://doi.org/10.1128/JVI.02391-15>.
74. Puck TT, Cieciora SJ, Robinson A. 1958. Genetics of somatic mammalian cells. III. Long-term cultivation of euploid cells from human and animal subjects. *J Exp Med* 108:945–956. <https://doi.org/10.1084/jem.108.6.945>.
75. Pertel PE, Fridberg A, Parish ML, Spear PG. 2001. Cell fusion induced by herpes simplex virus glycoproteins gB, gD, and gH-gL requires a gD receptor but not necessarily heparan sulfate. *Virology* 279:313–324. <https://doi.org/10.1006/viro.2000.0713>.
76. Krummenacher C, Baribaud I, Sanzo JF, Cohen GH, Eisenberg RJ. 2002. Effects of herpes simplex virus on structure and function of nectin-1/HveC. *J Virol* 76:2424–2433. <https://doi.org/10.1128/jvi.76.5.2424-2433.2002>.
77. Zhang N, Yan J, Lu G, Guo Z, Fan Z, Wang J, Shi Y, Qi J, Gao GF. 2011. Binding of herpes simplex virus glycoprotein D to nectin-1 exploits host cell adhesion. *Nat Commun* 2:577. <https://doi.org/10.1038/ncomms1571>.
78. Chowdary TK, Cairns TM, Atanasiu D, Cohen GH, Eisenberg RJ, Heldwein EE. 2010. Crystal structure of the conserved herpesvirus fusion regulator complex gH-gL. *Nat Struct Mol Biol* 17:882–888. <https://doi.org/10.1038/nsmb.1837>.